

Time Dependent Response of Polycarbonate and Microcellular Polycarbonate

GREGORY WING, ARUN PASRICHA, MARK TUTTLE, and VIPIN KUMAR*

Department of Mechanical Engineering, FU-10
University of Washington
Seattle, Washington 98195

Microcellular polycarbonate is a novel cellular material with cells on the order of $10\text{ }\mu\text{m}$ in diameter and a cell density on the order of 10^9 cells per cm^3 . In this study the room temperature creep response of microcellular polycarbonate is experimentally determined and compared with the creep behavior of polycarbonate. The viscoelastic response of polycarbonate and microcellular polycarbonate is characterized using Schapery's theory of nonlinear viscoelasticity. Polycarbonate exhibited a nonlinear creep response at stress levels above 24.13 MPa, while the nonlinear behavior in microcellular polycarbonate was initiated at lower stress levels. Creep strains of microcellular polycarbonate contain a significantly higher viscoplastic component compared with the unfoamed material.

INTRODUCTION

Microcellular polycarbonate is a novel polymeric foam material with cell diameters of approximately $10\text{ }\mu\text{m}$, and a bubble density as high as 5 to 10^9 cells per cubic centimeter (1). The large nucleation density allows one to achieve a significant reduction of material density, while maintaining the small average cell size. Microcellular polycarbonate foams with a wide range of densities have recently been produced by Kumar and co-workers (1,2) using carbon dioxide for nucleating the bubbles.

The microcellular structure is produced in a two-stage process, first used by Martini *et al.* to produce the microcellular structure in polystyrene (3). The first stage consists of saturating the polymer with a nonreacting gas in a room temperature pressure vessel. In the second stage the saturated polymer is removed from the pressure vessel and heated to its glass transition temperature for a predetermined period of time. Bubbles appear in the supersaturated polymer upon heating, and are limited in size by the high viscosity of the polymer near the glass transition temperature. At the appropriate time, the foamed polymer is quenched in room temperature water to prevent further bubble growth.

Since polymeric materials may exhibit an appreciable amount of creep at room temperature, the time dependent response of microcellular polycarbonate must be characterized before this material can be used in structural applications. The creep behavior of polymers may be linear or nonlinear, depending upon the material, the applied stress, and the load dura-

tion period. For most polymers, linear creep behavior is observed only at low stress levels and for short loading times. Thus, there is a need for a nonlinear viscoelastic theory to effectively characterize the creep of a polymer.

Single-integral representations have proven to be very attractive in describing the nonlinear viscoelastic behavior of materials. Most single-integral nonlinear theories are essentially modifications of the Boltzmann superposition integral. Findley's modified superposition principle (4), one example of a nonlinear single-integral constitutive equation, has been used extensively to describe the nonlinear behavior of various polymeric materials (4,5).

The single integral nonlinear theory utilized in the present study was developed by Schapery (6-9). Schapery's nonlinear viscoelastic theory has been derived from fundamental principles of irreversible thermodynamics, and has been successfully used in describing the behavior of polymers with and without fiber reinforcement (8,10-21). A thorough review of the thermodynamic basis of the Schapery theory has been provided by Hiel *et al.* (22). In this paper the creep response of polycarbonate and microcellular polycarbonate is fully characterized using Schapery's theory of nonlinear viscoelasticity. Creep response of microcellular polycarbonate was investigated for foams of relative densities (density of the foam divided by the density of polycarbonate) of 0.95 and 0.81, respectively.

THEORETICAL DEVELOPMENT

Most polymeric materials exhibit time dependent response to an applied load. In general, linear theo-

*To whom correspondence should be addressed.

ries of viscoelasticity provide an adequate representation of the material response at low stress levels and at low temperatures. Boltzmann superposition integral is one of the most popular means of describing the behavior of linear viscoelastic materials. For the case of uniaxial loading at a constant temperature, the Boltzmann superposition integral is given as:

$$\varepsilon(t) = A_0 \sigma + \int_0^t \Delta A(t-\tau) \frac{d\sigma}{d\tau} d\tau \quad (1)$$

where, $\varepsilon(t)$ is strain at current time t , A_0 is the instantaneous elastic compliance, and ΔA is the linear creep compliance function.

As with most polymeric materials, the viscoelastic behavior of foamed and unfoamed polycarbonate was found to be nonlinear. Data collected in this study are therefore being interpreted using Schapery's nonlinear theory.

The Schapery Theory

For the case of uniaxial loading at constant temperature, the Schapery theory reduces to the following single-integral expression.

$$\varepsilon(t) = g_0^t A_0 \sigma^t + g_1^t \int_0^t \Delta A(\psi - \psi') \frac{d(g_2^t \sigma^\tau)}{d\tau} d\tau \quad (2)$$

where

$$\psi = \int_0^t \frac{dt}{a_\sigma} \quad \text{and} \quad \psi' = \int_0^\tau \frac{d\tau}{a_\sigma}$$

In Eq 2, $\varepsilon(t)$, A_0 , and ΔA are defined as in Eq 1. g_0 , g_1 , g_2 , and a_σ are stress-dependent nonlinearizing parameters. The specific mathematical form of the linear creep compliance is not specified by the theory. In the present study the following creep compliance was used, as initially suggested by Schapery (8).

$$\Delta A(\psi) = \sum_{r=1}^N A_r [1 - e^{-\lambda_r \psi}] + D_f \psi \quad (3)$$

The terms A_r , λ_r , and D_f are all material constants. The exponential terms can be interpreted as representing a series of Kelvin elements and therefore represent viscoelastic behavior. The $D_f \psi$ term represents a steady flow component that results in an irrecoverable strain upon load removal and therefore represents viscoplastic behavior. Substituting Eq 3 into Eq 2 gives:

$$\begin{aligned} \varepsilon(t) = & g_0^t A_0 \sigma^t + g_1^t \int_0^t \left\{ \sum_{r=1}^N A_r [1 - e^{-\lambda_r (\psi - \psi')}] \right\} \\ & \times \frac{d(g_2^t \sigma^\tau)}{d\tau} d\tau + g_1^t \int_0^t D_f (\psi - \psi') \frac{d(g_2^t \sigma^\tau)}{d\tau} d\tau \end{aligned} \quad (4)$$

A recursive relation for the first two terms on the right-hand side of Eq 4, involving only the viscoelastic component of total strain, was obtained by Henriksen (20) and was subsequently implemented

by Roy and Reddy (19) and Ha and Springer (16). A similar recursive relation for the viscoplastic component was derived by Pasricha *et al* (10, 11) and was combined with the viscoelastic component to describe the viscoelastic-viscoplastic behavior of fiber-reinforced plastics. From data collected in this study it was deemed necessary to use a viscoelastic-viscoplastic constitutive model to describe the creep/creep-recovery behavior of polycarbonate and microcellular polycarbonate. The recursive relation obtained by integrating Eq 4 is:

$$\begin{aligned} \varepsilon(t) = & \left(g_0^t A_0 + g_1^t g_2^t \sum_{r=1}^N A_r - g_1^t g_2^t \sum_{r=1}^N A_r \beta_r^t \right) \sigma^t \\ & + g_1^t \left\{ \sum_{r=1}^N A_r \left[g_2^{t-\Delta t} \beta_r^t \sigma^{t-\Delta t} - e^{-\lambda_r \Delta \psi} q_r^{t-\Delta t} \right] \right\} \\ & + g_1^t D_f [p^{t-\Delta t} + 0.5(\psi^t - \psi^{t-\Delta t}) \\ & \times (g_2^t \sigma^t + g_2^{t-\Delta t} \sigma^{t-\Delta t})] \end{aligned} \quad (5)$$

A detailed description of the different parameters in the above equation can be found in (10, 11, 16, 19, 20).

Calculation of Viscoelastic Parameters

All the material parameters in Eq 5 can be obtained through a series of creep/creep-recovery tests. The stress history applied during such a test comprises a step load applied at the start of the test ($t = 0$) followed by a step unloading at time t_1 . During the creep time (i.e. for time $0 < t < t_1$), a constant load (σ_0) is applied and Eq 5 reduces to the following equation, as given by Pasricha, *et al* (10, 11):

$$\begin{aligned} \varepsilon_{\text{creep}}(t) = & \left(g_0^t A_0 + g_1^t g_2^t \sum_{r=1}^N A_r [1 - e^{-\lambda_r t/a_\sigma^t}] \right) \sigma_0 \\ & + (g_1^t g_2^t D_f t/a_\sigma^t) \sigma_0 \end{aligned} \quad (6)$$

Note that the values for g_0 , g_1 , g_2 , and a_σ are dependent upon the applied creep stress level σ_0 . At time ($t > t_1$) the load is removed and the creep recovery response is given by:

$$\begin{aligned} \varepsilon_{\text{recovery}}(t) = & g_2^t \sigma_0 \sum_{r=1}^N A_r [e^{-\lambda_r (t-t_1)} (1 - e^{-\lambda_r t_1/a_\sigma^t})] \\ & + (g_2^t D_f t_1/a_\sigma^t) \sigma_0 \end{aligned} \quad (7)$$

Linear viscoelastic behavior is usually observed at relatively low stress levels, and hence at these levels $g_0 = 1$, $g_1 = 1$, $g_2 = 1$, and $a_\sigma = 1$. Using these values, the creep equation Eq 6 reduces to:

$$\varepsilon_{\text{creep}}(t) = \left(A_0 + \sum_{r=1}^N A_r [1 - e^{-\lambda_r t}] \right) \sigma_0 + (D_f t) \sigma_0 \quad (8)$$

and the recovery equation Eq 7 reduces to:

$$\begin{aligned} \varepsilon_{\text{recovery}}(t) = & \sigma_0 \sum_{r=1}^N A_r [e^{-\lambda_r (t-t_1)} (1 - e^{-\lambda_r t_1})] \sigma_0 \\ & + (D_f t_1) \sigma_0 \end{aligned} \quad (9)$$

Nonlinear behavior is usually initiated at relatively high stress levels. In general at these higher stress levels $g_0 \neq 1$, $g_1 \neq 1$, $g_2 \neq 1$, $\alpha_r \neq 1$. To measure all the material parameters, creep/creep-recovery tests are carried out at linear and nonlinear stress levels. A stepwise listing of the material property evaluation procedure is given below:

a) The material constants A_r , λ_r , and D_f are obtained by numerical curve fitting of Eq 9 to the recovery data obtained from tests at linear stress levels.

b) The instantaneous compliance A_0 is determined by curve fitting Eq 8 to the creep data from tests at linear stress levels.

c) Nonlinearizing parameters are then determined using data from tests conducted at nonlinear stress levels where it is assumed that A_0 , A_r , λ_r , and D_f are already known. The nonlinearizing parameters g_2 and α_r are determined by curve fitting Eq 7 to the recovery data from tests conducted at nonlinear stress levels.

d) Nonlinearizing parameters g_0 and g_1 are then obtained by curve fitting Eq 6 to the creep data from tests at nonlinear stress levels.

EXPERIMENTAL PROCEDURE

Specimen Preparation

The experiments were performed using ASTM Type IV tensile specimens. The specimens were machined from a 1.57-mm-thick sheet of GE Plastics Lexan 9034 polycarbonate with a density of 1.20 g/cm³. The specimens were all produced with the same relative orientation in order to eliminate any effect of the extrusion induced anisotropy of the polycarbonate sheets. A photoelastic examination of the machined specimens was performed to verify that no significant residual stresses were produced during the machining process.

The microcellular foam tensile specimens were produced from premachined polycarbonate tensile specimens using the procedure of Kumar and Weller (1). This procedure basically entails saturating the polymer under high pressure with a nonreacting gas. Subsequent heating of the supersaturated polymer results in foaming by nucleation of gas-filled bubbles. The specific parameters of the foaming process are listed in Table 1 for the specimens used in this study.

Upon removal from the pressure vessel prior to foaming, the nucleating gas begins to diffuse out of the supersaturated specimen. This leaves the outer layer of the specimen with a relatively low concentration of the nucleating gas. Because of the low concentration of the nucleating gas in the outer layers, the

foaming process is limited to the interior regions of the specimen. This results in a specimen with a foamed core and an unfoamed integral skin. Kumar and Weller (23) have shown that the skin thickness of a foamed specimen is linearly proportional to the desorption time of the nucleating gas. For the present study the desorption time was between 10 and 20 min, producing a skin of approximately 40 μ m on the test specimen. The properties of the microcellular specimens produced for this study are given in Table 2. The density data in Table 2, and all creep data presented in this paper, are based on foam specimens with such an integral skin.

The relative densities reported for the foam specimens were determined using samples taken from the gage length of the tensile specimens.

Test Procedure

The creep/creep-recovery tests were conducted using dead weight tensile loading. Loads were applied to the specimen using an electric weight trolley car. The applied load history consisted of an 8-h creep period followed by 2-h recovery period.

Tensile creep tests were performed on polycarbonate and on microcellular polycarbonate. The microcellular polycarbonate specimens tested had relative densities 0.95 and 0.81. The polycarbonate was tested at six stress levels ranging from 13.79 to 51.71 MPa. The microcellular polycarbonate was tested at stress levels from 13.79 to 34.47 MPa for the 0.95 relative density foam, and from 13.79 to 27.58 MPa for the 0.81 relative density foam.

The strains in the test specimens were measured using an MTS model 632.11 extensometer monitored using a PC-based data acquisition system. The data acquisition system is capable of measuring strains as high as 0.374 m/m with a resolution of 0.0015 m/m. At every stress level and relative density of the foamed specimen at least three replicate tests were performed. All tests were performed at ambient room temperature and conditions.

RESULTS AND DISCUSSION

Polycarbonate

No measurable creep was observed in the unfoamed polycarbonate over the 8-h creep period at stress levels of 13.79 MPa or below. The viscoelastic behavior exhibited by polycarbonate between stress levels of 24.13 and 51.71 MPa was found to be highly nonlinear, and was characterized using Schapery's nonlinear viscoelastic theory.

The material constants A_0 , A_r , λ_r , and D_f are all determined at stress levels for which the material

Table 1. Processing Conditions for Microcellular Specimens.

Specimen Type	Saturation Pressure	Saturation Time	Foaming Temperature	Foaming Time
A	5.52 MPa	60 h	60°C	30 s
B	5.52 MPa	60 h	80°C	30 s

Table 2. Foam Properties for Microcellular Specimens.

Specimen Type	Foam Density	Relative Density	Average Cell Dia. (2)	Cell Density (2) Cells/cm ³
A	1.14 g/cm ³	0.95	1.6 μ m	6.37×10^9
B	0.97 g/cm ³	0.81	2.5 μ m	8.38×10^9

exhibits linear viscoelastic behavior. An isochronous stress-strain curve using strain data obtained at 1 min and 470 min from the initial loading time was used to determine the stress level at which nonlinear behavior is initiated. The isochronous curve for polycarbonate is shown in Fig. 1. On the basis of these results, the creep response of polycarbonate was considered linear at stress levels of 24.13 MPa and below.

The material property values for polycarbonate obtained using the above constitutive equations are listed below. Four pairs of A_r , λ_r were used in the exponential series expansion employed to characterize the linear viscoelastic compliance.

1) Linear compliance values:

$$\begin{aligned} A_0 &= 3.9671\text{E-}04 \\ A_1 &= 4.5704\text{E-}06 & \lambda_1 &= 0.001 \\ A_2 &= 1.9165\text{E-}05 & \lambda_2 &= 0.01 \\ A_3 &= 1.4419\text{E-}05 & \lambda_3 &= 0.1 \\ A_4 &= 2.2354\text{E-}05 & \lambda_4 &= 1.0 \end{aligned}$$

Where A_r has units of MPa^{-1} , λ_r has units of min^{-1} .

2) Flow parameter:

$$D_f = 1.4966\text{E-}08$$

D_f has units of $\text{min}^{-1} \text{MPa}^{-1}$.

3) Nonlinearizing parameters:

$$\begin{aligned} g_0(\sigma) &= 1 + 0.002650\exp(\sigma/10.13) \\ g_1(\sigma) &= 1 + 0.014752\exp(\sigma/11.77) \\ g_2(\sigma) &= 1 + 0.029063\exp(\sigma/12.05) \\ a_r(\sigma) &= 1 - 0.013946\exp(\sigma/12.86) \end{aligned}$$

Where the applied stress σ has units of MPa.

Creep and recovery data from tests performed at several stress levels and the curve fits obtained using the material property values listed above are shown in Fig. 2. From the recovery strain data shown in Fig. 2 it is evident that a significant amount of total strain induced in the 8-h creep time is viscoplastic (i.e. irrecoverable) strain.

Microcellular Polycarbonate

Microcellular foams of relative densities 0.95 and 0.81 were each tested at four different stress levels ranging from 13.79 to 34.47 MPa, and 13.79 to 27.58 MPa, respectively. For the foamed specimens, a significant creep response was observed at all stress levels considered. The lowest stress levels used were treated as linear stress levels for the microcellular foams. Because of difficulties encountered in producing tensile specimens free of geometric distortion, tests could not be conducted on foams of relative density lower than 0.81.

It was attempted to evaluate the material properties for microcellular polycarbonate using the material evaluation procedure outlined above. During the material property evaluation for the microcellular

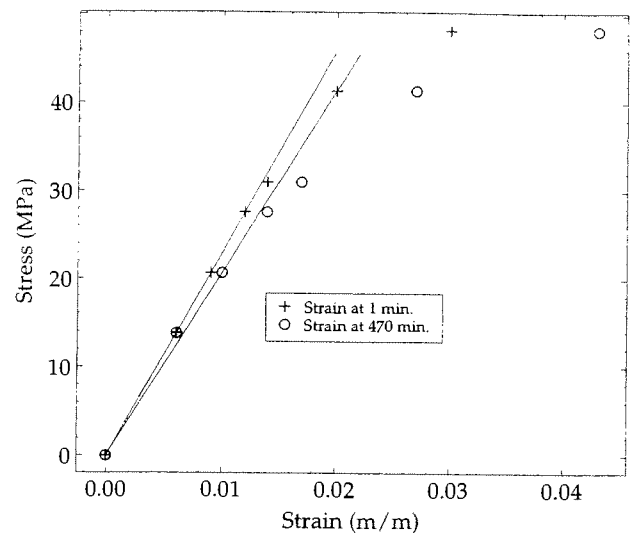


Fig. 1. Isochronous curves for solid polycarbonate at 1 min and 470 min.

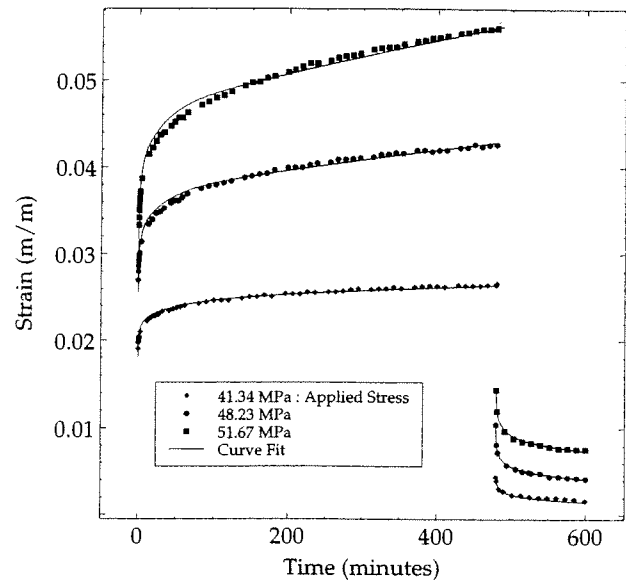


Fig. 2. Creep/creep recovery response of polycarbonate.

foam, it was determined that the flow term does not adequately model the creep/creep-recovery behavior of foams. The flow term results in a linear increase in the viscoplastic strain with loading time, which was not experimentally observed. This is evidenced in Figs. 4 and 5, where it is seen that the slope of the total strain vs. time curve during the loading period is less than the slope that would be required for the linear flow term to produce the viscoplastic strain observed after 8 h of loading. The above constitutive model, therefore, underestimates the viscoplastic strains at higher stress levels. A constant strain term, k , was therefore added to the nonlinear recovery equation (Eq 7) in the curve fitting procedure.

The nonlinear recovery equation used for the microcellular foams is:

$$\varepsilon_{\text{recovery}}(t) = g_2^t \sigma_0 \sum_{r=1}^N A_r [e^{-\lambda_r(t-t_1)}(1 - e^{-\lambda_r t_1 a_v^t})] + (g_2^t D_f t_1 / a_v^t) \sigma_0 + k \quad (10)$$

Use of the modified nonlinear recovery equation (Eq 10) to evaluate the microcellular foam property values led to a change in the property evaluation procedure previously listed. The material property evaluation procedure for the microcellular foams is listed below:

a) The material constants A_0 , A_r , λ_r , and D_f are obtained by numerical curve fitting of Eq 8 to the creep data obtained from tests at linear stress levels.

b) Nonlinearizing parameters are determined using data from tests conducted at nonlinear stress levels where it is assumed that A_0 , A_r , λ_r , and D_f are already known. The nonlinearizing parameters g_0 , a_v , and the product $g_1 g_2$ are determined by curve fitting Eq 6 to the creep data from the tests conducted at nonlinear stress levels.

c) Nonlinearizing parameter g_2 is then obtained by curve fitting Eq 10 to the recovery data from tests conducted at nonlinear stress levels. During the curve fitting of Eq 10 the strain offset term k is also determined.

d) Nonlinearizing parameter g_1 is obtained by dividing the product $g_1 g_2$ obtained in step b by g_2 determined step c.

It should be pointed out that there is no thermodynamic basis for the constant k , and it was used to offset the inadequacy of the linear flow term in modeling the viscoplastic behavior of microcellular foam. Figure 3 shows a plot of the underestimated viscoplastic strain, k , for various loads. The material property values for the microcellular foams using the above procedure are listed below:

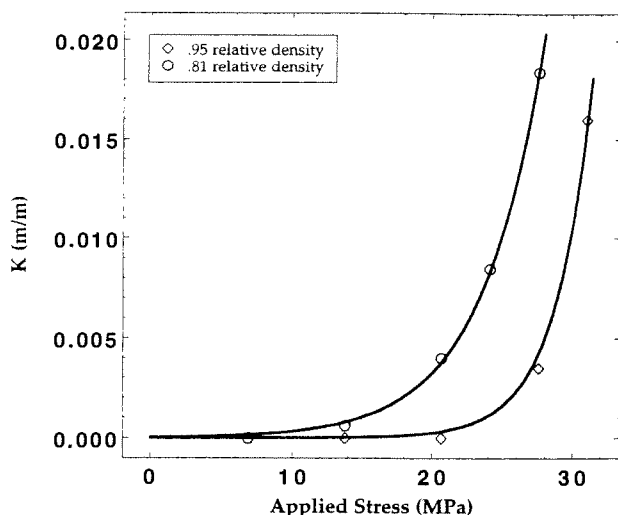


Fig. 3. Underestimated viscoplastic strain, k , for the 0.95 and 0.81 relative density foams.

0.95 Relative Density Microcellular Foam

1) Linear compliance values:

$$\begin{aligned} A_0 &= 4.689\text{E-}04 \\ A_1 &= 7.066\text{E-}06 & \lambda_1 &= 0.001 \\ A_2 &= 1.457\text{E-}04 & \lambda_2 &= 0.01 \\ A_3 &= 4.908\text{E-}05 & \lambda_3 &= 0.1 \\ A_4 &= 1.527\text{E-}05 & \lambda_4 &= 1.0 \end{aligned}$$

Where A_r has units of MPa^{-1} , λ_r has units of min^{-1} .

2) Flow parameter:

$$D_f = 1.35\text{E-}07$$

D_f has units of $\text{min}^{-1} \text{MPa}^{-1}$.

3) Nonlinearizing parameters:

$$\begin{aligned} g_0(\sigma) &= 1 + 2.14\text{E-}04 \exp(\sigma/4.49) \\ g_1(\sigma) &= 1 + 1.434\text{E-}05 \exp(\sigma/2.81) \\ g_2(\sigma) &= 1 + 6.72\text{E-}03 \exp(\sigma/7.73) \\ a_v(\sigma) &= 1 - 5.1\text{E-}03 \exp(\sigma/7.32) \end{aligned}$$

Where the applied stress σ has units of MPa.

0.81 Relative Density Microcellular Foam

1) Linear compliance values:

$$\begin{aligned} A_0 &= 6.889\text{E-}04 \\ A_1 &= 2.108\text{E-}05 & \lambda_1 &= 0.001 \\ A_2 &= 1.927\text{E-}04 & \lambda_2 &= 0.01 \\ A_3 &= 9.290\text{E-}05 & \lambda_3 &= 0.1 \\ A_4 &= 2.263\text{E-}05 & \lambda_4 &= 1.0 \end{aligned}$$

Where A_r has units of MPa^{-1} , λ_r has units of min^{-1} .

2) Flow parameter:

$$D_f = 1.511\text{E-}07$$

D_f has units of $\text{min}^{-1} \text{MPa}^{-1}$.

3) Nonlinearizing parameters:

$$\begin{aligned} g_0(\sigma) &= 1 + 2.46\text{E-}05 \exp(\sigma/2.82) \\ g_1(\sigma) &= 1 + 3.12\text{E-}03 \exp(\sigma/4.65) \\ g_2(\sigma) &= 1 + 4.52\text{E-}09 \exp(\sigma/1.70) \\ a_v(\sigma) &= 1 - 1.89\text{E-}03 \exp(\sigma/5.07) \end{aligned}$$

Where the applied stress σ has units of MPa.

Figures 4 and 5 show the creep/creep-recovery strain data and the curve fits obtained using the material properties for the 0.95 and 0.81 relative density foams, respectively. Figure 6 shows a plot of g_0 , one of the nonlinearizing parameters, for polycarbonate and microcellular polycarbonate.

The creep recovery of the microcellular foams (Figs. 4 and 5) contain a much higher amount of viscoplastic strain than polycarbonate (Fig. 2). Figure 7 shows

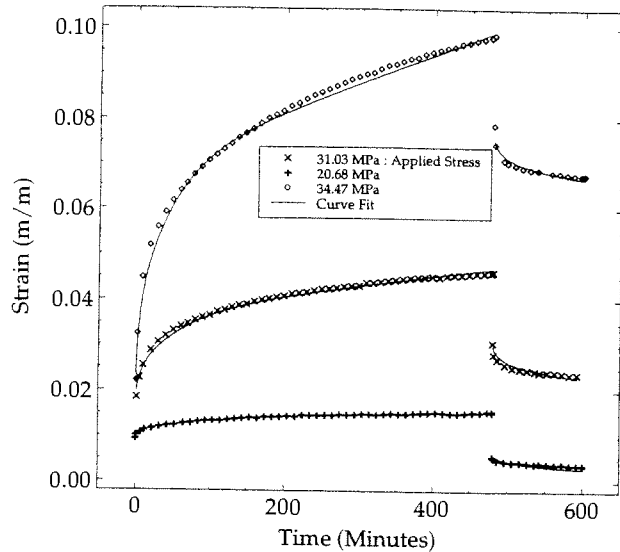


Fig. 4. Creep/creep recovery response of 0.95 relative density microcellular polycarbonate foam.

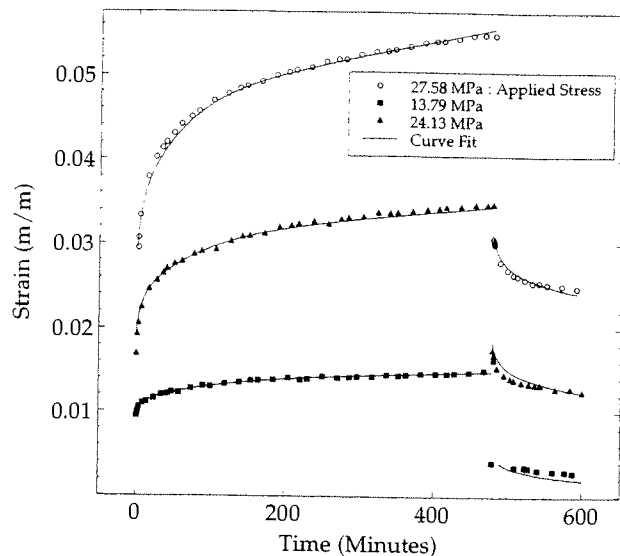


Fig. 5. Creep/creep recovery response of 0.81 relative density microcellular polycarbonate foam.

the creep response of the foamed and unfoamed polycarbonate subjected to identical stress loads. From Fig. 7 it is seen that the viscoelastic/viscoplastic response of the foamed polycarbonate is of greater magnitude for the same stress load. It is also evident from Fig. 7 that as the foam density is decreased, the instantaneous compliance (A_0) of the microcellular polycarbonate does not decrease as rapidly as the viscoelastic compliance. This important material response is also easily seen in Fig. 8, which compares the instantaneous strain to the strain after the 8-h creep period for the tests shown in Fig. 7.

In polycarbonate, the maximum tensile strain at initiation of creep rupture is approximately 7.2% (24).

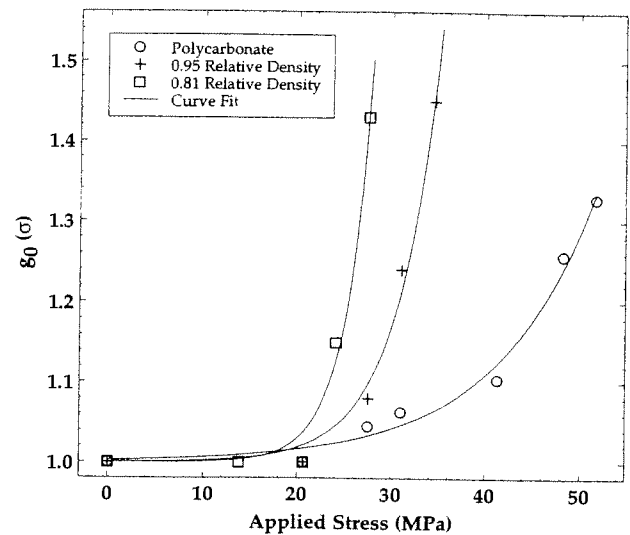


Fig. 6. Variation of g_0 with applied stress for foamed and unfoamed polycarbonate.

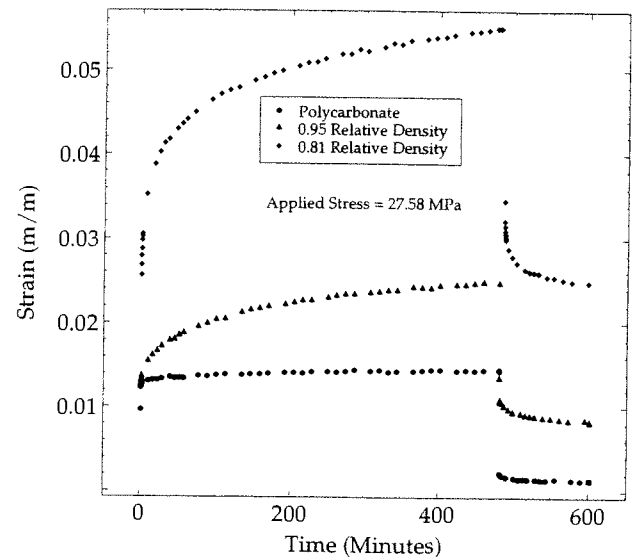


Fig. 7. Creep response of foamed and unfoamed polycarbonate subjected to identical stress loads.

However, microcellular polycarbonate foams of both 0.95 and 0.81 relative density were crept to strains well in excess of this amount with no signs of creep rupture initiation. This is illustrated in Fig. 4 for a 0.95 relative density foam subjected to an applied stress of 34.47 MPa. Thus it appears that microcellular polycarbonate foams can undergo much larger strains, compared with polycarbonate, before creep rupture initiates.

CONCLUSIONS

The creep response of microcellular polycarbonate initiates at lower stress levels compared with polycarbonate. The creep response of the foams is greater in

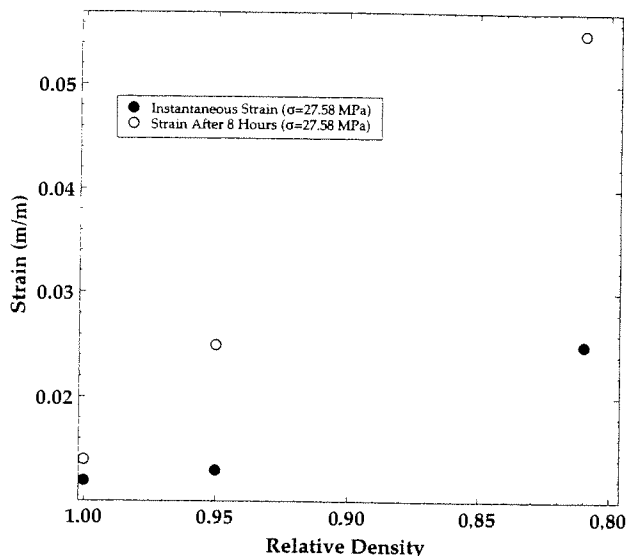


Fig. 8. Instantaneous strain and strain after 8-h creep loading for foamed and unfoamed polycarbonate subjected to identical loads.

magnitude for a given stress level than that of polycarbonate. The viscoplastic strain at the end of the creep period represents a much higher percentage of the total strain for the foams than for the polycarbonate. It also appears that microcellular polycarbonate foams can undergo much larger strains, compared with polycarbonate, before creep rupture initiates.

The room temperature creep response of polycarbonate and microcellular polycarbonate was characterized using Schapery's theory of nonlinear viscoelasticity in this study. The viscoplastic response was also modeled by the use of a flow term in the linear compliance. The flow term based constitutive model was found to adequately model the viscoelastic/viscoplastic response of polycarbonate. This constitutive model, however, grossly underestimated the viscoplastic component of strain for the microcellular polycarbonate at high stress levels. A viscoplastic strain, k , was added to the 8-h viscoplastic prediction of the linear flow term to offset this underprediction. A more complex viscoplastic constitutive model is therefore required for modeling the creep/creep-recovery response of microcellular foams.

ACKNOWLEDGMENTS

This research was funded by National Science Foundation grant MSS 9114840, a grant from the Washington Technology Centers, and by the UW-Industry Cellular Composites Consortium. This support is gratefully acknowledged.

NOMENCLATURE

- A_0 = Instantaneous compliance.
- ΔA = Linear viscoelastic compliance.
- A_r = Component of linear viscoelastic compliance.
- D_f = Component of linear viscoelastic compliance.
- λ_r = Component of linear viscoelastic compliance.
- $\varepsilon(t)$ = Strain at time t .
- E_0 = Instantaneous Young's modulus.
- g_0 = Nonlinearizing parameter.
- g_1 = Nonlinearizing parameter.
- g_2 = Nonlinearizing parameter.
- a_σ = Nonlinearizing parameter.
- σ^t = Stress at time t .
- Ψ = Reduced time.

REFERENCES

1. V. Kumar and J. E. Weller, *SPE ANTEC Tech. Papers*, **37**, 1401 (1991).
2. V. Kumar and M. VanderWel, *SPE ANTEC Tech. Papers*, **37**, 1406 (1991).
3. J. E. Martini-Vvedensky, N. P. Suh, and F. A. Waldman, U.S. Patent No. 4,473,665 (1984).
4. W. N. Findley, and J. S. Y. Lai, *Trans. Soc. Rheol.*, **2**, 361 (1967).
5. D. A. Dillard, M. R. Straight, and H. F. Brinson, *Polym. Eng. Sci.*, **27**, 114 (1987).
6. R. A. Schapery, *Proc. 5th U.S. Nat. Cong. Appl. Mech.*, ASME (1966).
7. R. A. Schapery, *Purdue University Report*, AA&ES 69-2, Feb. 1969.
8. R. A. Schapery, *Polym. Eng. Sci.*, **9**, 295 (1969).
9. R. A. Schapery, *Proc. IUTAM Symposium East Kilbride*, June 1968.
10. A. Pasricha, P. Van Duser, M. E. Tuttle, and A. F. Emery, *Proc. VII Int. Cong. Experimental Mechanics*, pp. 35-43 (1992).
11. A. Pasricha, M. E. Tuttle, and A. F. Emery, *Proc. ASC 7th Tech. Conf. Compos. Mat.*, pp. 792-803 (1992).
12. M. E. Tuttle, and H. F. Brinson, *NASA Contract Report 3371* (March 1985).
13. M. E. Tuttle, and H. F. Brinson, *Exp. Mech.*, **26**, 89 (1986).
14. Y. C. Lou and R. A. Schapery, *J. Compos. Mater.*, **5**, 208 (1971).
15. R. Mohan and D. F. Adams, *Exp. Mech.*, **25**, 262 (1985).
16. S. K. Ha and G. S. Springer, *J. Compos. Mater.*, **23**, 1159 (1989).
17. D. Peretz and Y. Weitsman, *J. Rheol.*, **26**, 245 (1982).
18. D. E. Walrath, *Exp. Mech.*, **31**, 111 (1991).
19. S. Foy and J. N. Reddy, *Computers Structures*, **29**, 1011 (1988).
20. M. Henriksen, *Computers Structures*, **18**, 133 (1987).
21. D. A. Dillard, M. R. Straight, and H. F. Brinson, *Polym. Eng. Sci.*, **27**, 114 (1987).
22. C. C. Hiel, A. H. Cardon, and H. F. Brinson, *VPI & SU Report*, VPI-E-83-6 (March 1983).
23. V. Kumar and J. E. Weller, *SPE ANTEC Tech. Papers*, **38**, 1508 (1992).
24. M. J. Mindel and N. Brown, *J. Mater. Sci.*, **8**, 863 (1973).

Received April 29, 1993

Revision received September 1993